



## Article

# The Effect of Excessive Sulfate in the Li-Ion Battery Leachate on the Properties of Resynthesized $\text{Li}[\text{Ni}_{1/3}\text{Co}_{1/3}\text{Mn}_{1/3}]\text{O}_2$

Jimin Lee <sup>1</sup>, Sanghyuk Park <sup>1</sup>, Mincheol Beak <sup>1</sup>, Sang Ryul Park <sup>2</sup>, Ah Reum Lee <sup>2</sup>, Suk Hyun Byun <sup>2</sup>, Junho Song <sup>3,\*</sup>, Jeong Soo Sohn <sup>4,\*</sup>  and Kyungjung Kwon <sup>1,\*</sup> 

<sup>1</sup> Department of Energy and Mineral Resources Engineering, Sejong University, 209 Neungdong-ro, Gwangjin-gu, Seoul 05006, Korea; txoio7612@naver.com (J.L.); shpark@sejong.ac.kr (S.P.); doqmsalscjf@naver.com (M.B.)

<sup>2</sup> SungEel HiTech Co., Ltd., 143-12, Gunsansandan-ro, Gunsan-si 54002, Korea; qkrtkdfuf68@sungeel.com (S.R.P.); ahreum@sungeel.com (A.R.L.); shbn14@sungeel.com (S.H.B.)

<sup>3</sup> Korea Electronics Technology Institute, 25 Saenari-ro, Bundang-gu, Seongnam-si 13509, Korea

<sup>4</sup> Mineral Resources Research Division, Resources Recovery Research Center, Korea Institute of Geoscience and Mineral Resources, 124, Gwahak-ro Yuseong-gu, Daejeon 34132, Korea

\* Correspondence: junesong@keti.re.kr (J.S.); jss@kigam.re.kr (J.S.S.); kfromberk@gmail.com (K.K.); Tel.: +82-2-3408-3947 (K.K.)

**Abstract:** In order to examine the effect of excessive sulfate in the leachate of spent Li-ion batteries (LIBs),  $\text{LiNi}_{1/3}\text{Co}_{1/3}\text{Mn}_{1/3}\text{O}_2$  (pristine NCM) and sulfate-containing  $\text{LiNi}_{1/3}\text{Co}_{1/3}\text{Mn}_{1/3}\text{O}_2$  (NCMS) are prepared by a co-precipitation method. The crystal structures, morphology, surface species, and electrochemical performances of both cathode active materials are studied by scanning electron microscopy (SEM), X-ray diffraction (XRD), X-ray photoelectron spectroscopy (XPS), and charge-discharge tests. The XRD patterns and XPS results identify the presence of sulfate groups on the surface of NCMS. While pristine NCM exhibits a very dense surface in SEM images, NCMS has a relatively porous surface, which could be attributed to the sulfate impurities that hinder the growth of primary particles. The charge-discharge tests show that discharge capacities of NCMS at C-rates, which range from 0.1 to 5 C, are slightly decreased compared to pristine NCM. In  $dQ/dV$  plots, pristine NCM and NCMS have the same redox overvoltage regardless of discharge C-rates. The omnipresent sulfate due to the sulfuric acid leaching of spent LIBs has a minimal effect on resynthesized NCM cathode active materials as long as their precursors are adequately washed.

**Keywords:** Li-ion battery; cathode material; sulfate; impurity; leachate



**Citation:** Lee, J.; Park, S.; Beak, M.; Park, S.R.; Lee, A.R.; Byun, S.H.; Song, J.; Sohn, J.S.; Kwon, K. The Effect of Excessive Sulfate in the Li-Ion Battery Leachate on the Properties of Resynthesized  $\text{Li}[\text{Ni}_{1/3}\text{Co}_{1/3}\text{Mn}_{1/3}]\text{O}_2$ . *Materials* **2021**, *14*, 6672. <https://doi.org/10.3390/ma14216672>

Academic Editor: Alberto Vertova

Received: 16 September 2021

Accepted: 3 November 2021

Published: 5 November 2021

**Publisher's Note:** MDPI stays neutral with regard to jurisdictional claims in published maps and institutional affiliations.



**Copyright:** © 2021 by the authors. Licensee MDPI, Basel, Switzerland. This article is an open access article distributed under the terms and conditions of the Creative Commons Attribution (CC BY) license (<https://creativecommons.org/licenses/by/4.0/>).

## 1. Introduction

Li-ion batteries (LIBs) have been extensively used in various portable electronics and electric vehicles in combination with high energy and power density [1,2]. However, tremendous amounts of end-of-life batteries have been piled up in landfill, and flammable and toxic elements in spent LIBs would cause not only fire but also soil contamination [3–5]. At the same time, the spent LIBs could also offer huge economic benefits by recovering valuable elements in them [6,7]. In respect of LIB composition, there are many portions of valuable metals including cobalt, nickel, and lithium. When the spent LIBs are treated properly, worthy elements such as cobalt and lithium can be regained. From the viewpoint of economic and environmental issue, the recycling of spent LIBs is essential for the present and future generation [8].

In the recycling process of batteries, the pretreatment of spent batteries, including discharge, dismantling, classification, and separation, usually precedes the hydrometallurgy-based recycling process [9]. The hydrometallurgy-based process involves a leaching step to extract desired metals from cathode materials by using leaching agents such as sulfuric acid [10]. A large number of research articles have investigated the leaching behaviors of metals in the spent LIBs, with the optimization of the leaching step leading to the

maximization of leaching efficiencies for valuable metals. [11–14]. Because sulfuric acid leaching is the most popular in LIB recycling and usual metal sources for the synthesis of LIB cathode active materials are sulfate salts such as  $\text{NiSO}_4$ ,  $\text{CoSO}_4$ , and  $\text{MnSO}_4$ , the investigation on the effect of sulfate in pristine and resynthesized cathode active materials would be essential.

Previously, Ban et al. found that sulfur in  $\text{LiNi}_x\text{Co}_y\text{Mn}_z\text{O}_2$  (NCM) enhanced the electrochemical performance of the cathode active materials, in which sulfur was incorporated into NCM by calcination [15]. Interestingly, discharge capacity and rate capability were improved with the small amount of sulfur doping (0.4 and 0.5 wt%), which is contrary to the common sense of LIB industry that sulfur is a harmful impurity. The authors explained the reason being that sulfur forms a  $\text{Li}_2\text{SO}_4$  phase, which would provide fast diffusion channels for lithium ions on the surface. Recently, Li et al. examined the concentration gradient S-doped NCM and argued that a proper amount of sulfate stabilizes the crystal structure with good cycle performance [16]. However, these studies first prepared precursors for NCM by co-precipitation and conducted the sulfur doping by calcination, which is unlikely in the NCM resynthesis for LIB recycling, because the leachate for the subsequent co-precipitation of NCM already contains excessive sulfate. Therefore, the effect of sulfur in NCM, especially in the case of NCM resynthesis, should be investigated with S-doped NCM that is prepared by co-precipitation.

In this work, we synthesize  $\text{LiNi}_{1/3}\text{Co}_{1/3}\text{Mn}_{1/3}\text{O}_2$  (pristine NCM) and sulfate-containing  $\text{LiNi}_{1/3}\text{Co}_{1/3}\text{Mn}_{1/3}\text{O}_2$  (NCMS) using co-precipitation in order to investigate the effect of excessive sulfate in the leachate for the NCM resynthesis. Since an actual LIB leachate could contain various types of unidentified impurities, we prepare a simulated LIB leachate with 4 M of extra lithium sulfate as a sulfur source. Our previous report, on the effect of residual lithium in resynthesized NCM, revealed that lithium originating from lithium sulfate in a simulated leachate hardly affects the LIB performance as long as the NCM precursors are washed appropriately [17]. Thus, we could attribute the properties of NCMS, which was prepared from the simulated LIB leachate with extra lithium sulfate, to sulfate in the leachate. The structural characterization is performed by scanning electron microscopy (SEM), X-ray diffraction (XRD), and X-ray photoelectron spectroscopy (XPS). For electrochemical performance, we fabricate CR2032-type coin cells using a Li metal foil as anode to measure charge and discharge capacities at different C-rates, which range from 0.1 to 5 C.

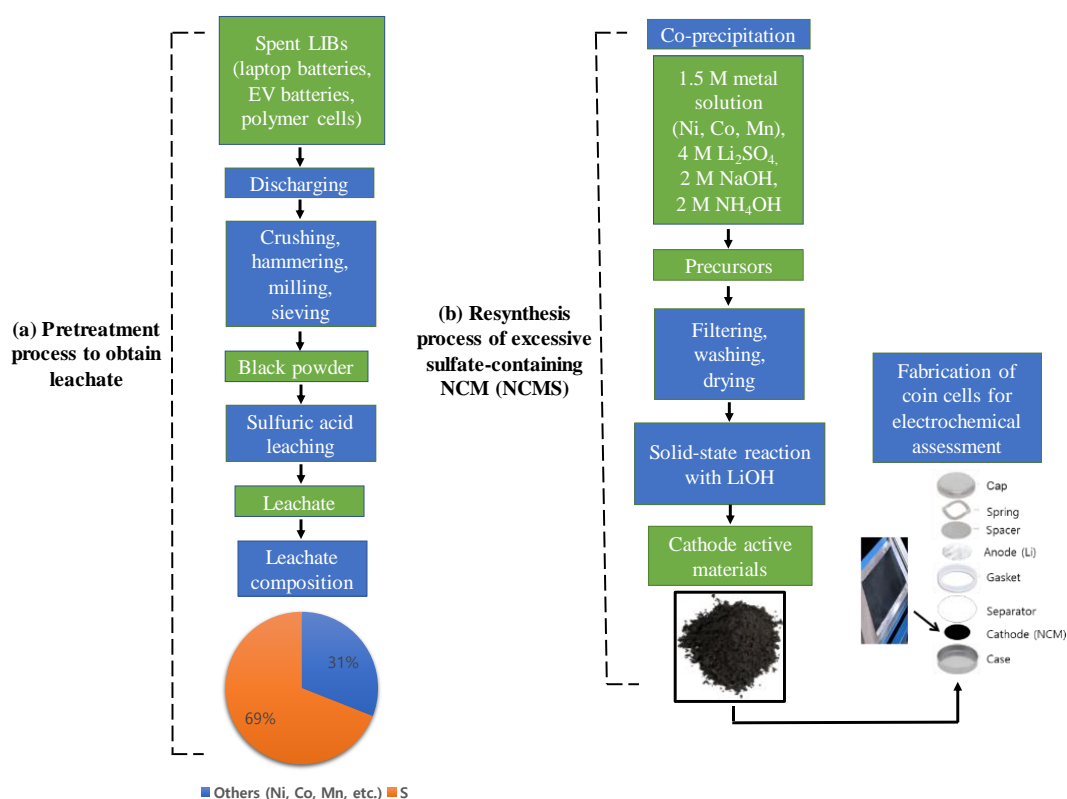
## 2. Experimental Section

Figure 1 shows the flowchart of methodology simulating a resynthesis process of excessive sulfate-containing NCM from leachate of spent LIBs, which include cylindrical 18650 laptop batteries, electric vehicle batteries, and polymer cells. Incidentally, the spent LIBs are mainly composed of graphite as anode material, and  $\text{LiCoO}_2$  and NCM as cathode materials.

### 2.1. Synthesis and Characterization of Materials

$\text{Ni}_{1/3}\text{Co}_{1/3}\text{Mn}_{1/3}(\text{OH})_2$  and sulfate-containing  $\text{Ni}_{1/3}\text{Co}_{1/3}\text{Mn}_{1/3}(\text{OH})_2$  were synthesized using the co-precipitation method. The composition of actual leachate of spent LIBs from a LIB recycling company (SungEel HiTech, Gunsan-si, Korea) was considered to simulate the amount of sulfur in the actual leachate. A total of 2 M of ammonia solution as a chelating agent and 1.5 M of metal solution ( $\text{NiSO}_4 \cdot 6\text{H}_2\text{O}$ ,  $\text{CoSO}_4 \cdot 7\text{H}_2\text{O}$ , and  $\text{MnSO}_4 \cdot \text{H}_2\text{O}$  in 1:1:1 mole ratio with 4 M of extra  $\text{Li}_2\text{SO}_4$  (99%, Alfa Aesar, Ward Hill, MA, USA)) were pumped into a continuous stirred reactor. 2 M of NaOH solution was automatically injected into the reactor by a pH-controlled pump to maintain a pH of 11.52. The reactor was kept at a temperature of 40 °C and a stirring speed of 1000 rpm for about 75 h. The resultant precursors were filtered and washed with distilled water several times and dried in an oven at 80 °C. The final cathode active materials (pristine NCM and NCMS) were prepared by calcinating a mixture of the hydroxide precursors and  $\text{Li}_2\text{CO}_3$  as a lithium source at

1000 °C for 8 h under air atmosphere. In order to identify the crystal structure of the NCM and NCMS materials, an XRD technique (X'Pert, PAN analytical, Cu K $\alpha$  radiation, Almelo, The Netherlands) was carried out with a step size of 0.026° in a 2 $\theta$  range from 10° to 80°. The morphological characterization of the materials was performed using a field emission SEM (FE-SEM, SU-8010, Hitachi Ltd., Tokyo, Japan). XPS (K-Alpha 1063, Thermo Fisher Scientific, Waltham, MA, USA) was used to examine the presence of sulfur in the structure of NCMS.



**Figure 1.** Flowchart of methodology for the resynthesis of excessive sulfate-containing NCM from spent LIBs. (a) Typical pretreatment process of spent LIBs with subsequent acidic leaching process using H<sub>2</sub>SO<sub>4</sub>, indicating the excessive sulfur content in leachate. (b) Synthesis process of sulfate-containing NCMS(OH)<sub>2</sub> precursors using the co-precipitation method and NCMS cathode active materials via a solid-state reaction, followed by a fabrication of coin cells for electrochemical assessment.

## 2.2. Electrochemical Analysis

Electrochemical properties were investigated using CR2032-type coin cells, which were fabricated in a moisture-controlled glove box under argon atmosphere. Cathodes were prepared by mixing the cathode active materials, polyvinylidene fluoride (KF 1100) binder, and carbon black (Super-P) in a mass ratio of 95:3:2 respectively. Cells were integrated with the prepared cathodes, lithium metal as an anode, polyethylene film as a separator, and 1 M LiPF<sub>6</sub> in a mixture of ethyl methyl carbonate and ethylene carbonate (2:1 volume ratio) as an electrolyte. Charge-discharge tests were performed from 3.0 to 4.3 V (vs. Li/Li<sup>+</sup>) at room temperature.

## 3. Results and Discussion

Figure 2 shows the content of various elements in the actual LIB leachate from a LIB recycling company (SungEel HiTech, Gunsan-si, Korea). Li, Ni, Mn, and Co are detected as major constituents of cathode materials and other metal elements, including Al, Cu, and Na, originate from current collectors and the pretreatments for LIB recycling [18–20]. Notably, nonmetal elements, including F, Cl, and S, are detected in the LIB leachate. Each

element was analyzed by the following methods: Inductively coupled plasma for metal elements, absorptiometric analysis using La alizarin complexone for F,  $\text{AgNO}_3$  titration for Cl, and barium sulfate precipitation for S. F can originate from residual electrolytes such as  $\text{LiPF}_6$  [21], and Cl might derive from the discharging process using NaCl [22]. Since sulfuric acid is commonly used for leaching LIBs, a great amount of S is present in the leachate and S has the highest concentration among all the elements [23]. This suggests that the influence of S on the LIB performance of resynthesized cathode active materials needs to be investigated.

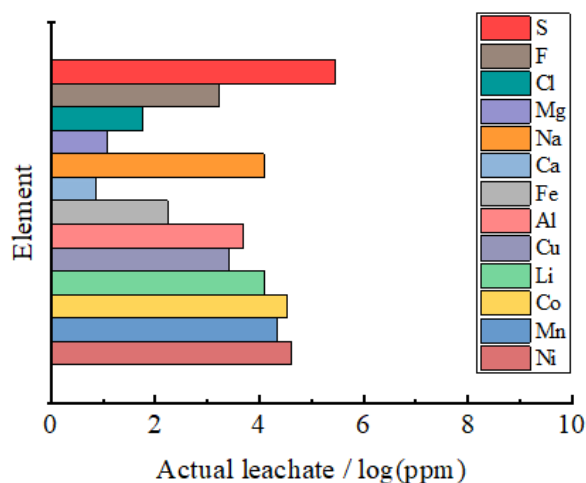


**Figure 2.** The content of various elements in the actual LIB leachate.

The SEM images in Figure 3 show the morphology of the precursors of pristine NCM and NCMS according to the co-precipitation time. Both precursors have spherical secondary particles consisting of needle-like primary particles, with an average secondary particle diameter of  $\sim 10 \mu\text{m}$ . The particles grow bigger and more spherical as the co-precipitation time increases. Compared with pristine NCM, which has the continuous particle growth with decreasing particulates, NCMS shows sluggish particle growth after 64 h. Besides, NCMS has a relatively porous surface even when the co-precipitation appears to stop, while pristine NCM exhibits a very dense surface. This may attribute to the sulfate impurities that hinder the growth of primary particles.

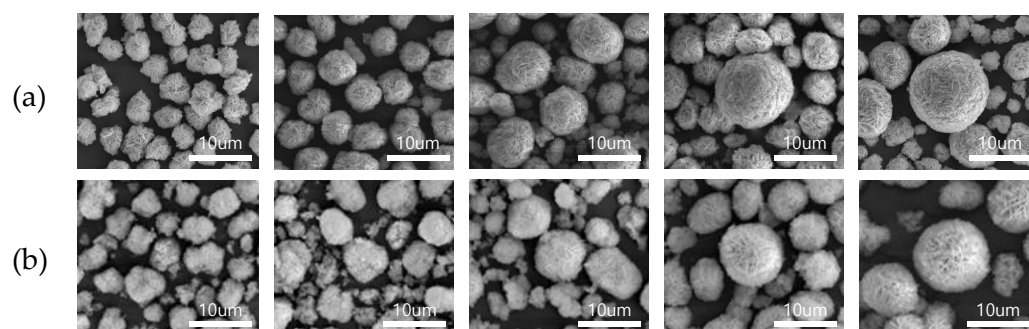


**Figure 3.** SEM images of the precursors of (a) pristine NCM and (b) NCMS according to the co-precipitation time ((a) 16, 24, 40, 64, and 72 h, (b) 5, 26, 40, 64, and 75 h).

Figure 4 shows the SEM images of the cathode active materials of pristine NCM and NCMS. The difference between pristine NCM and NCMS is more distinct in the cathode active materials than their precursors. NCMS, whose precursors have porous surface, is likely to have more voids and its primary particles agglomerate more than pristine NCM during the calcination step. This may cause the structure instability and deteriorate the electrochemical performance [24]. Besides, larger primary particles decrease the lithium-ion

conductivity due to their longer diffusion paths [25]. These results suggest that excessive sulfate affects the surface morphology of NCM, which could exert a noticeable influence on the LIB performance.

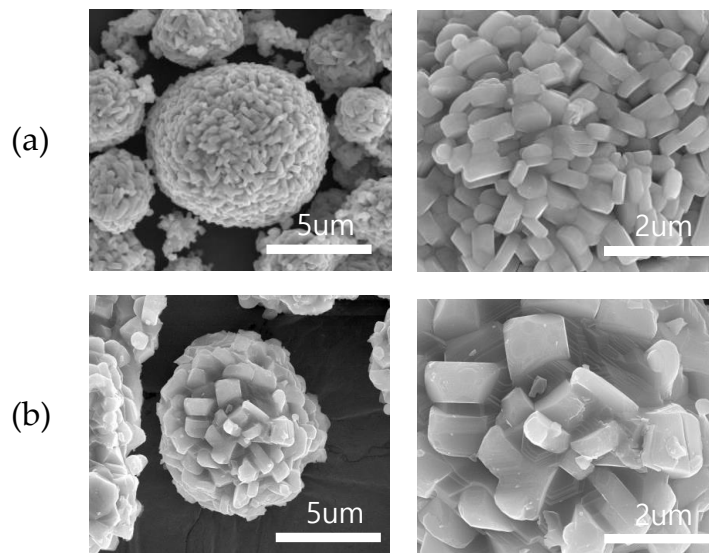


**Figure 4.** SEM images of the cathode active materials of (a) pristine NCM and (b) NCMS.

Figure 5a shows that all diffraction peaks are well consistent with  $\beta$ -Ni(OH)<sub>2</sub> with no impurity phase [26]. There is no distinct difference between pristine NCM and NCMS in the precursors. Figure 5b reveals that both pristine NCM and NCMS have the well-layered structure of  $\alpha$ -NaFeO<sub>2</sub> type with the space group  $R\bar{3}m$  [27,28]. However, an Li<sub>2</sub>SO<sub>4</sub> impurity phase around 22° peak is observed in NCMS. This result indicates that some sulfate impurities are still present in the precursors after filtering and washing, and these sulfate impurities appear in the cathode active materials after calcination and could lead to poor performance in a charge-discharge test. These weak peaks related to Li<sub>2</sub>SO<sub>4</sub> phase are also proven by the presence of sulfur in the following XPS analysis (Figure 6). Figure 6b exhibits a binding energy of 169.2 eV, which is assigned to hexavalent S 2p<sub>3/2</sub> of the SO<sub>4</sub><sup>2-</sup> groups [29]. This result identifies the presence of sulfate groups on the surface of NCMS.

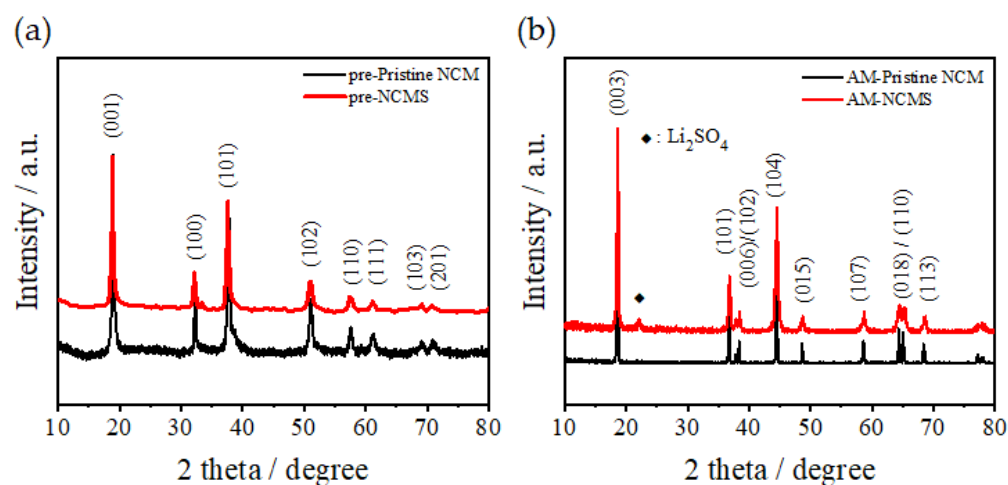


**Figure 5.** XRD patterns of the (a) precursors and (b) cathode active materials of pristine NCM and NCMS.

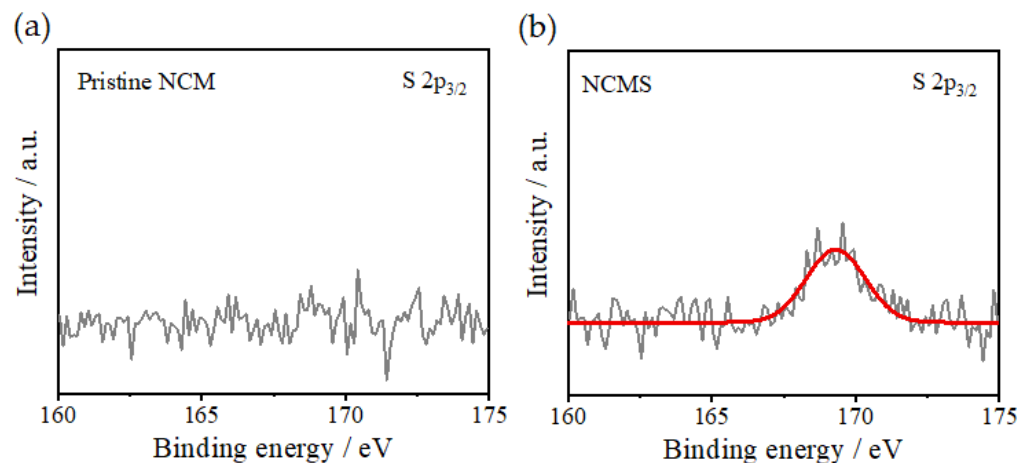


**Figure 6.** XPS profiles of the cathode active materials of (a) pristine NCM and (b) NCMS.

The electrochemical performance of the charge-discharge profiles for pristine NCM and NCMS is presented in Figure 7a. For both samples, the C-rate during the charge was fixed at 0.1 C, while the C-rates during the discharge were varied from 0.1 to 5 C. Compared to pristine NCM, the discharge capacities of NCMS at each C-rate is slightly decreased. The discharge capacities at 0.1 C are 161.1 and 159.6 mAh g<sup>-1</sup> for pristine NCM and NCMS, respectively. During the initial charge to 4.3 V vs. Li/Li<sup>+</sup>, a gentle slope below 3.9 V occurs with the removal of lithium from NCM, which accompanies the oxidation of Ni<sup>2+</sup>/Ni<sup>4+</sup> and Co<sup>3+</sup>/Co<sup>4+</sup> [15]. Although the presence of sulfate was confirmed in the structural characterizations of NCMS, the decrease in its discharge capacity is not significant. The coulombic efficiencies are 99.4% and 99.7% at 0.1 C, 89.7% and 89.0% at 2 C, and 82.7% and 79.6% at 5 C for pristine and NCMS, respectively. These results indicate that excessive sulfate in NCM has a minimal effect on the reversibility in the Ni and Co redox system. The dQ/dV plots of pristine NCM and NCMS at 0.1, 2, and 5 C were obtained to examine the reversibility and redox overvoltage of the cathode active materials (Figure 7b). Both samples at 0.1 C display the reduction and oxidation peaks of Ni<sup>4+</sup>/Ni<sup>2+</sup> at 3.74 and 3.76 V, respectively. The reduction peaks gradually shift to lower potentials as the C-rate during the discharge increases. However, the difference in the position of reduction peaks is very small between pristine NCM and NCMS. The capacity retention of pristine NCM and NCMS cycled at 1 C showed superior cyclability over 98% after 50 cycles in both samples (see Figure S1). Therefore, considering that pristine NCM and NCMS have the same redox overvoltage and the cycle stability, the sulfate groups belonging to NCM would not seriously affect the reversibility of the cathode active materials.

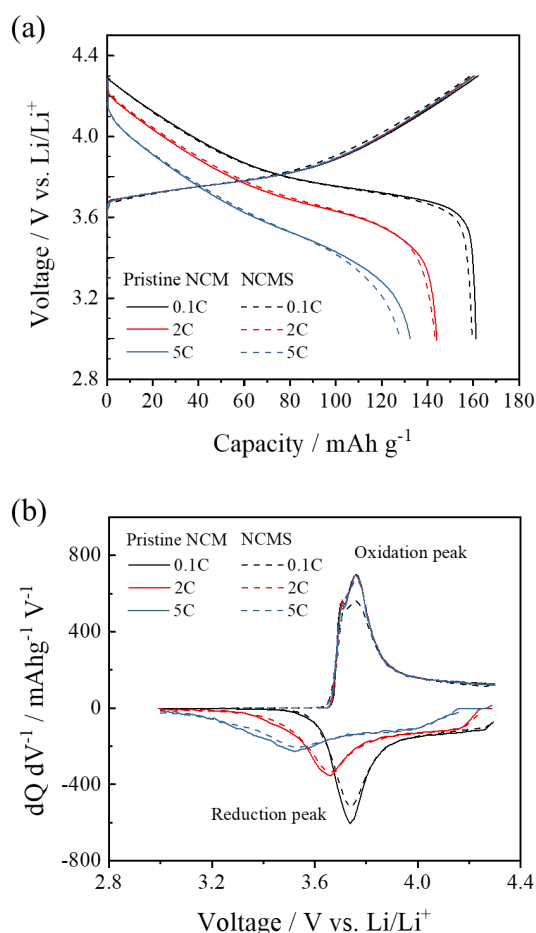


**Figure 7.** (a) Charge and discharge capacities and (b)  $dQ/dV$  plots of pristine NCM and NCMS at 0.1, 2, and 5 C.

#### 4. Conclusions

In this work, pristine NCM and NCMS are synthesized by co-precipitation and the effect of excessive sulfate is investigated on their structure, morphology, and electrochemical properties. The presence of sulfate in NCMS is examined by XRD and XPS results. SEM results show that NCMS has a porous surface and more voids than pristine NCM, which may cause the structural instability and deteriorate the electrochemical performance. In charge-discharge tests at different C-rates, the discharge capacities of NCMS at each C-rate is slightly decreased compared to pristine NCM. In summary, the unavoidable presence of sulfate, which originates from the sulfuric acid leaching of spent LIBs, has a minimal effect on resynthesized NCM cathode active materials as long as their precursors are adequately washed.

**Supplementary Materials:** The following are available online <https://www.mdpi.com/article/10.3390/ma14216672/s1>, Figure S1: Capacity retention of pristine NCM and NCMS at 1 C.

**Author Contributions:** Conceptualization, S.P. and S.H.B.; methodology, M.B., S.R.P. and A.R.L.; validation, S.R.P., A.R.L. and S.H.B.; investigation, S.P. and M.B.; writing—original draft preparation, J.L. and K.K.; writing—review and editing, J.L. and J.S.; supervision, J.S.S. and K.K.; project administration, J.S. and J.S.S. All authors have read and agreed to the published version of the manuscript.

**Funding:** This work was supported by the Technology Innovation Program (20011176) funded By the Ministry of Trade, Industry & Energy (MOTIE, Korea), and K. Kwon was supported by Basic Science Research Program through the National Research Foundation of Korea (NRF) funded by the Ministry of Education (2020R1A6A1A03038540).

**Institutional Review Board Statement:** Not applicable.

**Informed Consent Statement:** Not applicable.

**Data Availability Statement:** The data presented in this study are available on request from the corresponding author.

**Conflicts of Interest:** The authors declare no conflict of interest.

## References

1. Manthiram, A. An outlook on lithium ion battery technology. *ACS Cent. Sci.* **2017**, *3*, 1063–1069. [[CrossRef](#)]
2. Li, W.; Erickson, E.M.; Manthiram, A. High-nickel layered oxide cathodes for lithium-based automotive batteries. *Nat. Energy* **2020**, *5*, 26–34. [[CrossRef](#)]
3. Xu, J.; Thomas, H.R.; Francis, R.W.; Lum, K.R.; Wang, J.; Liang, B. A review of processes and technologies for the recycling of lithium-ion secondary batteries. *J. Power Sources* **2008**, *177*, 512–527.
4. Zeng, X.; Li, J.; Ren, Y. Prediction of various discarded lithium batteries in China. In Proceedings of the 2012 IEEE International Symposium on Sustainable Systems and Technology (ISSST), Boston, MA, USA, 16–18 May 2012; pp. 1–4.
5. Contestabile, M.; Panero, S.; Scrosati, B. A laboratory-scale lithium-ion battery recycling process. *J. Power Sources* **2001**, *92*, 65–69.
6. Ku, H.; Jung, Y.; Jo, M.; Park, S.; Kim, S.; Yang, D.; Rhee, K.; An, E.; Sohn, J.; Kwon, K. Recycling of spent lithium-ion battery cathode materials by ammoniacal leaching. *J. Hazard. Mater.* **2016**, *313*, 138–146. [[CrossRef](#)]
7. Bruce, R.C. The role of hydrometallurgy in achieving sustainable development. *Hydrometallurgy* **1992**, *30*, 1–28.
8. Yang, Y.; Sun, W.; Bu, Y.; Zhang, C.; Song, S.; Hu, Y. Recovering valuable metals from spent lithium ion battery via a combination of reduction thermal treatment and facile acid leaching. *ACS Sustain. Chem.* **2018**, *6*, 10445–10453.
9. Kim, S.; Bang, J.; Yoo, J.; Shin, Y.; Bae, J.; Jeong, J.; Kim, K.; Dong, P.; Kwon, K. A comprehensive review on the pretreatment process in lithium-ion battery recycling. *J. Clean. Prod.* **2021**, *294*, 126329. [[CrossRef](#)]
10. Harper, G.; Sommerville, R.; Kendrick, E.; Driscoll, L.; Slater, P.; Stolkin, R.; Walton, A.; Christensen, P.; Heidrich, O.; Lambert, S.; et al. Recycling lithium-ion batteries from electric vehicles. *Nature* **2019**, *575*, 75–86. [[CrossRef](#)]
11. Li, D.F.; Wang, C.Y.; Yin, F.; Chen, Y.Q.; Yang, Y.Q.; Jie, X.W. Carbon reduction of lithium cobalt dioxide and its dissolution in sulfuric acid solution. *Nonferrous Met.* **2009**, *61*, 83–86.
12. Meshram, P.; Pandey, B.D.; Mankhand, T.R. Hydrometallurgical processing of spent lithium ion batteries (LIBs) in the presence of a reducing agent with emphasis on kinetics of leaching. *Chem. Eng. J.* **2015**, *281*, 418–427. [[CrossRef](#)]
13. Meshram, P.; Pandey, B.D.; Mankhand, T.R. Process optimization and kinetics for leaching of rare earth metals from the spent Ni-metal hydride batteries. *Waste Manag.* **2016**, *51*, 196–203. [[CrossRef](#)]
14. Zhang, P.; Yokoyama, T.; Itabashi, O.; Suzuki, T.M.; Inoue, K. Hydrometallurgical process for recovery of metal values from spent lithium-ion secondary batteries. *Hydrometallurgy* **1998**, *47*, 259–271. [[CrossRef](#)]
15. Ban, L.; Yin, Y.; Zhuang, W.; Lu, H.; Wang, Z.; Lu, S. Electrochemical performance improvement of  $\text{Li}_{1.2}[\text{Mn}_{0.54}\text{Ni}_{0.13}\text{Co}_{0.13}]\text{O}_2$  cathode material by sulfur incorporation. *Electrochim. Acta* **2015**, *180*, 218–226. [[CrossRef](#)]
16. Li, J.; Wu, J.; Li, S.; Liu, G.; Cui, Y.; Dong, Z.; Liu, H.; Sun, X. Stabilizing  $\text{LiNi}_{0.8}\text{Co}_{0.15}\text{Mn}_{0.05}\text{O}_2$  cathode by doping sulfate for lithium-ion batteries. *ChemSusChem* **2021**, *14*, 2721–2730. [[CrossRef](#)] [[PubMed](#)]
17. Jo, M.; Ku, H.; Park, S.; Song, J.; Kwon, K. Effects of residual lithium in the precursors of  $\text{Li}[\text{Ni}_{1/3}\text{Co}_{1/3}\text{Mn}_{1/3}]\text{O}_2$  on their lithium-ion battery performance. *J. Phys. Chem. Solids* **2018**, *118*, 47–52. [[CrossRef](#)]
18. Kim, S.; Park, S.; Jo, M.; Beak, M.; Park, J.; Jeong, G.; Yu, J.; Kwon, K. Electrochemical effects of residual Al in the resynthesis of  $\text{Li}[\text{Ni}_{1/3}\text{Mn}_{1/3}\text{Co}_{1/3}]\text{O}_2$  cathode materials. *J. Alloys Compd.* **2021**, *857*, 157581.
19. Jo, M.; Park, S.; Song, J.; Kwon, K. Incorporation of Cu into  $\text{Li}[\text{Ni}_{1/3}\text{Co}_{1/3}\text{Mn}_{1/3}]\text{O}_2$  cathode: Elucidating its electrochemical properties and stability. *J. Alloys Compd.* **2018**, *764*, 112–121. [[CrossRef](#)]
20. Beak, M.; Park, S.; Kim, S.; Park, J.; Jeong, S.; Thirumalraj, B.; Jeong, G.; Kim, T.; Kwon, K. Effect of Na from the leachate of spent Li-ion batteries on the properties of resynthesized Li-ion battery cathodes. *J. Alloys Compd.* **2021**, *873*, 159808. [[CrossRef](#)]
21. Wang, Q.; Jiang, L.; Yu, Y.; Sun, J. Progress of enhancing the safety of lithium ion battery from the electrolyte aspect. *Nano Energy* **2019**, *55*, 93–114.
22. Xiao, J.; Guo, J.; Zhan, L.; Xu, Z. A cleaner approach to the discharge process of spent lithium ion batteries in different solutions. *J. Clean. Prod.* **2020**, *255*, 120064. [[CrossRef](#)]
23. Tang, X.; Tang, W.; Duan, J.; Yang, W.; Wang, R.; Tang, M.; Li, J. Recovery of valuable metals and modification of cathode materials from spent lithium-ion batteries. *J. Alloys Compd.* **2021**, *874*, 159853.
24. Chen, D.; Kramer, D.; Mönig, R. Chemomechanical fatigue of  $\text{LiMn}_{1.95}\text{Al}_{0.05}\text{O}_4$  electrodes for lithium-ion batteries. *Electrochim. Acta* **2018**, *259*, 939–948. [[CrossRef](#)]
25. Wagner, A.C.; Bohn, N.; Geßwein, H.; Neumann, M.; Osenberg, M.; Hilger, A.; Manke, I.; Schmidt, V.; Binder, J.R. Hierarchical structuring of NMC111-cathode materials in lithium-ion batteries: An in-depth study on the influence of primary and secondary particle sizes on electrochemical performance. *ACS Appl. Energy Mater.* **2020**, *3*, 12565–12574. [[CrossRef](#)]
26. Guan, X.Y.; Deng, J.C. Preparation and electrochemical performance of nano-scale nickel hydroxide with different shapes. *Mater. Lett.* **2007**, *61*, 621–625.



27. Wang, B.; Zhang, F.-L.; Zhou, X.-A.; Wang, P.; Wang, J.; Ding, H.; Dong, H.; Liang, W.-B.; Zhang, N.-S.; Li, S.-Y. Which of the nickel-rich NCM and NCA is structurally superior as a cathode material for lithium-ion batteries? *J. Mater. Chem. A* **2021**, *9*, 13540. [[CrossRef](#)]
28. Xu, G.; Li, J.; Xue, Q.; Dai, Y.; Zhou, H.; Xindong, W.; Kang, F. Elevated electrochemical performance of  $(\text{NH}_4)_3\text{AlF}_6$ -coated  $0.5\text{Li}_2\text{MnO}_3 \cdot 0.5\text{LiNi}_{1/3}\text{Co}_{1/3}\text{Mn}_{1/3}\text{O}_2$  cathode material via a novel wet coating method. *Electrochim. Acta* **2014**, *117*, 41–47. [[CrossRef](#)]
29. Nefedov, V.-I. A comparison of results of an ESCA study of nonconducting solids using spectrometers of different constructions. *J. Electron. Spectrosc. Relat. Phenom.* **1982**, *25*, 29–47. [[CrossRef](#)]